mm-Wave on Wheels: Practical 60 GHz Vehicular Communication Without Beam Training

Adrian Loch[†] Arash Asadi[♭] Gek Hong Sim[♭] Joerg Widmer[†] Matthias Hollick [♭]
[♭]Technische Universität Darmstadt, Germany
[†]IMDEA Networks Institute, Madrid, Spain

***Abstract*—At vehicular speeds, the contact time during which a mobile node is in range of a fixed road side unit (RSU) is short. While this is not an issue if the RSU only needs to deliver textual information such as traffic updates, short contact times become problematic when transmitting a large amount of information. For instance, an RSU may need to deliver high volumes of local navigation data for an augmented reality application, or video material regarding tourist information of a nearby town. Millimeter-wave (mm-Wave) communication is highly promising for such scenarios since it provides order-of-magnitude larger throughput than the existing technologies operating at lower frequencies. However, the contact time in mm-Wave vehicular scenarios becomes even shorter due to the directional nature of the communication. This raises a fundamental question: can the high throughput of mm-Wave make up for the reduction in the contact time? In this paper, we analyze this trade-off and design a first-of-its-kind practical mm-Wave vehicular testbed to evaluate the resulting performance. Specifically, we consider alternative locations for the RSU other than at the side of the road, such as on top of a bridge or inside a roundabout. Moreover, we leverage that the road implicitly determines the direction in which the RSU expects a car to be located. This allows us to use fixed beam-steering at both the car and the RSU, thus avoiding costly beam-training. We validate our approach in real-world vehicular scenarios with actual traffic in a mid-sized town in Spain. The results show that our fixed beam-steering approach enables the RSU to transmit large amounts of data in a very short amount of time for a wide range of speeds. This allows us to provide detailed insights into the aforementioned fundamental question regarding the use of mm-Wave in vehicular scenarios.**

I. Introduction

The amount of data generated and consumed in vehicular scenarios has moved from lightweight textual information (e.g., traffic updates) to vast multimedia and sensor data [1]. Existing vehicular network protocols such as IEEE 802.11p only achieve up to 27 Mbps and thus do not provide enough bandwidth to support such applications. To solve this bottleneck, recent work suggests using millimeter-wave (mm-Wave) bands [2], which can achieve multi-gigabit-per-second performance. Moreover, it can be successfully combined with other vehicular systems in that band such as radar [3]. The key problem of communication in the mm-Wave band is that at such frequencies attenuation is extremely high. As a result, mm-Wave transceivers typically must use directional antennas to overcome this effect. In highly mobile scenarios such as vehicular networks, this poses a number of critical questions:

1) How can transceivers perform efficient beam-steering at vehicular speeds such that they always reach each other?

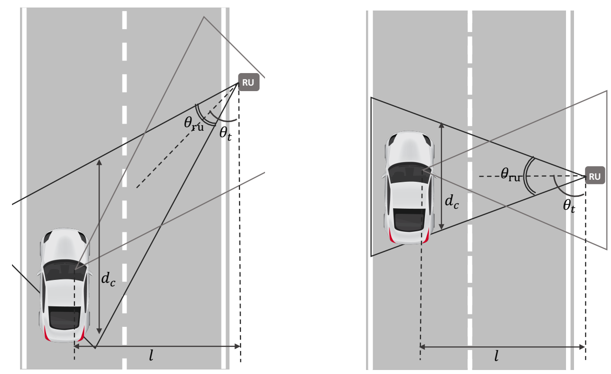

(a) RSU at 45°. (b) RSU at 90°.

Fig. 1: Vehicular mm-Wave communication toy scenario.

2) Where shall mm-Wave antennas be located on cars? Since the car itself acts as a blockage at mm-Wave frequencies, an antenna placed on one side cannot cover the other side. A simple solution is to place the antenna on a pole on top of the car but this would strongly disagree with aesthetic considerations of car manufacturers, and may cause safety, air resistance, and noise issues.
3) How wide shall the beamwidth of the mm-Wave antennas on a car be? While narrow values allow for greater range, this also requires more frequent beamsteering.
4) How much data can transceivers exchange in a mobile scenario? Given the limited range at mm-Wave frequencies and the directional nature of the communication, the contact time between transceivers is likely short.

In this paper, we provide answers to the above questions in practice using a first-of-its-kind mm-Wave vehicular testbed operating in the 60 GHz band. Specifically, we consider an infrastructure to vehicle scenario, where Road Side Units (RSUs) transmit data to vehicles. This data includes contents such as video material of nearby points of interest, live video feeds of traffic at locations with low visibility (e.g., sharp road bends), or infotainment services (e.g., delivery of large data volumes requested by passengers). For this scenario, we propose an approach that eliminates the use of beamsteering by leveraging the characteristics of vehicular communications. Given the fact that cars on a road always approach the RSU from the same direction, one can estimate a suitable fix antenna location, orientation, and beamwidth to maximize the throughput within the short contact time. Fig. 1 depicts a toy scenario of our approach on a one-way double-lane street. Instead of using costly beam-training to point a narrow beam towards the car as in Fig. 1a and then tracking its movement until the location in Fig. 1b, we claim that using a fix antenna configuration is a simple yet effective approach that achieves high performance at a fraction of the system complexity. That is, instead of tracking the movement of cars to provide a continuous connection, we just deliver bursts of information while a car is within the static beam of an RSU. With this approach, we address all of the four aforementioned questions. Specifically, our contributions are as follows:

- We propose a simple yet effective approach to select a fixed antenna steering for multiple RSU scenarios such as at the road side, on a bridge, and in a roundabout.
- We study the impact of antenna beamwidth in the above RSU scenarios, and analytically optimize it.
- We address the impact of reflectors in vehicular scenarios, such as the walls of buildings or cars parked nearby.
- We validate our approach in a practical vehicular testbed operating at 60 GHz. Our results provide insights into metrics such as throughput, signal-to-noise ratio (SNR), bit error rate (BER), and packet error rate (PER).

The remainder of this paper is structured as follows. In Section II, we review related work on mm-Wave vehicular communications. Next, we describe and discuss our fixed beam steering and antenna placement approach in Section III. We then introduce our vehicular 60 GHz testbed in Section IV, and present our experimental results in Section V. Finally, we conclude the paper in Section VI.

II. Related Work

While mm-Wave communication is envisioned to play a key role in vehicular networks [1], [2], [4], related work in this area is limited. The authors of [3] theoretically show that mm-Wave 60 GHz communication using the 802.11ad standard is a viable candidate for automotive radars [3]. However, they do not analyze the performance of 802.11ad in a vehicular setting but focus on how to use it for car detection. In fact, the body of work on experimental analysis of mmWave is very limited [5]–[11]. The majority of the work does not focus on vehicular communication [5]–[8]. In [9] and [10], the authors perform channel measurements in the 60 GHz band for links within a car and from the car to a unit located outside. Both consider static scenarios only, and thus only account for the impact of the car structure on the communication. In contrast, we analyze the influence of speed on crucial metrics such as SNR, BER, and PER under real-world traffic conditions. Most importantly, [9], [10] are limited to channel measurements. That is, they do not take into account the effects of actual data transmission involving, for instance, frame detection, coding, and modulation. Recent work [11] studies these aspects for mm-Wave mobile networks, including vehicular scenarios. However, [11] focuses on the design of a frame structure for cellular mm-Wave networks operating at 28 GHz. While the authors develop and implement a real-time vehicular testbed, they only carry out two basic experiments and do not consider actual traffic. Moreover, they place the antenna on top of the vehicle to prevent shadowing by the car itself. As discussed in Section I, this is highly unrealistic. In contrast, we analyze the impact of placing the antenna inside the vehicle, and perform an extensive evaluation in multiple scenarios considering a broad range of parameters. This sets our work apart from [11].

Beyond vehicular applications, research on mm-Wave communication focuses on channel characterization. This is key to understand whether networks operating in the mm-Wave band are feasible. Transmission in the mm-Wave band is shown to achieve multi-gigabit-per-second rates, and may thus solve once and for all the capacity issue in cellular and WiFi networks [7]. Studies in this area characterize and define the mm-Wave communication link and transmission challenges, respectively. One of those challenges is the high atmospheric attenuation in the mm-Wave band. Related work thoroughly studies the impact of climate on the quality of mm-Wave links [12]–[14]. In [13], Hao *et al.* determine the multipath and time varying channel behaviour of 38 GHz radio links for various weather events and provide design guidelines to model a mm-Wave wireless communication system. Further, [14] and [12] also characterize the impact of climate on mm-Wave links but focus on rainfall for 35 GHz and 60 GHz, respectively. While we perform our vehicular measurement campaign under good weather conditions only, recent practical work shows that 60 GHz links can operate reliably also in case of rain [15].

Related work also explores the unique features as well as the vulnerability of directional mm-Wave links. For instance, Sur *et al.* perform an in-depth indoor measurement characterizing the coverage, bit-rate, beam steering impact, blockage, and spatial reuse of 60 GHz links using a software-radio platform [16]. Further, [5], [17]–[19] emphasize on the importance of beam switching and alignment in face of signal degradation or signal loss. These issues become critical with high mobility. To address them, we leverage that cars typically follow predictable mobility patterns. The above work mostly conducts measurements for propagation characterization in static and quasi-static scenarios. In contrast, we focus on validating the feasibility of exploiting high data rate transmissions within a very short transmission time in highly mobile scenarios.

III. System Model

In the following, we describe the RSU scenarios that we consider in this paper. Moreover, we analytically study the impact of the antenna steering angle and the antenna beamwidth on the contact time. We define the contact time as the time during which the RSU and the in-car-unit (ICU) can exchange data. In this paper, we consider infrastructure to vehicle communication, that is, the RSU is the transmitter and the ICU is the receiver. The contact time among both is directly related to the speed of the car and the distance that the car travels within the beam of the transmitter. We model this time based on geometric considerations for three RSU cases—at the road side, on top of a bridge, and within a roundabout.

A. RSU at the Road Side

Our first scenario focuses on an RSU located at the road side and pointing towards arriving traffic at an angle of θ_t, as shown in Fig. 1a. For our model, we assume that the ICU uses the same antenna configuration as the RSU, that is, it also steers at an angle of θ_t. Next, we show how to select both the transmit beamwidth at the RSU θ_{rsu}, and the direction of transmission θ_t that result in the largest contact time. Let the antenna beamwidth at the RSU be θ_{rsu}. The contact distance between the RSU and ICU for $0° < \theta_t < 90°$ is:

$$d_c(\theta_t, \theta_{\text{rsu}}) = l\left(\frac{1}{\tan\left(90° - \theta_t - \frac{\theta_{\text{rsu}}}{2}\right)} - \tan\left(\theta_t - \frac{\theta_{\text{rsu}}}{2}\right)\right), \quad (1)$$

where l is the horizontal distance between the RSU and the ICU. The contact time is directly related to the speed at which the vehicle is driving v_{icu}, and can be written as:

$$t_c(\theta_t, \theta_{\text{rsu}}) = \frac{d_c(\theta_t, \theta_{\text{rsu}})}{v_{\text{icu}}}. \quad (2)$$

For $\theta_t = 90°$, as depicted in Fig. 1b, the contact time is:

$$t_c(\theta_t = 90°, \theta_{\text{rsu}}) = \frac{2l\tan\left(\frac{\theta_{\text{rsu}}}{2}\right)}{v_{\text{icu}}}. \quad (3)$$

We do not consider angles $\theta_t > 90°$. This would mean transmitting data to the car while it is moving away from the RSU, which results in equivalent contact times compared to the case when the car is moving towards the RSU. As an example, we compare the contact time for $\theta_t = 45°$ and $\theta_t = 90°$, similar to our toy scenario in Fig. 1. If the antenna beamwidth at the RSU is $\theta_{\text{rsu}} = 20°$, we can easily compute that the contact time for $\theta_t = 45°$ is more than twice that of $\theta_t = 90°$. For a wider beamwidth such as $\theta_{\text{rsu}} = 80°$, the benefit of using $\theta_t = 45°$ is even larger. Specifically, $t_c(45°, \theta_{\text{rsu}}) > 6 \times t_c(90°, \theta_{\text{rsu}})$. However, while a wider beamwidth may provide a longer contact time, it may also result in lower transmit rates since the antenna gain typically decreases with the antenna beamwidth. Thus, we formulate the optimal θ_t^* and θ_{rsu}^* which jointly maximize the contact time and the transmission rate $R_m(\theta_t, \theta_{\text{rsu}})$ between the transmitter and the RSU as in Eq. 4.

$$\theta_t^*, \theta_{\text{rsu}}^* = \arg\max_{\theta_t, \theta_{\text{rsu}}} t_c(\theta_t, \theta_{\text{rsu}}) R_m(\theta_t, \theta_{\text{rsu}}) \quad (4)$$

Placing the RSU at the road side can result in reflections, as shown in Fig. 2. For instance, a row of parked cars can result in the signal reaching an arriving car even before the car enters the direct beam of the RSU. As a result, the car would receive the signal in two bursts—the first one when crossing the reflection and the second one when crossing the direct beam. This increases the contact time and may thus be beneficial in some scenarios. In our evaluation in Section V, we analyze in practice whether such a case is possible. However, we do not model this case analytically since it involves elements which are out of control of the network operator, such as the location of parked cars. While the operator could place dedicated reflectors at the road side to achieve this effect, we consider this to be out of scope of this paper.

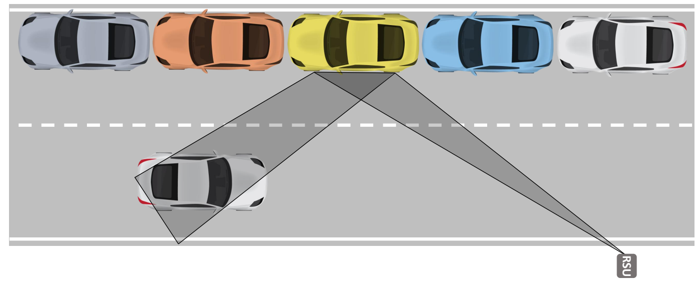

Fig. 2: Car reflection case. The row of cars are parked cars.

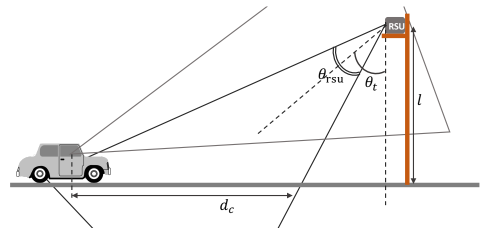

Fig. 3: RSU located at the top of a bridge.

B. RSU on Top of a Bridge

Our second scenario considers an RSU located at the top of a bridge. The benefit of this location is that cars on the road cannot cause blockage. For instance, in Fig. 1, a car driving on the right line would block the signal from the car driving on the left. In contrast, if the signal reaches the cars from above, all of them can receive it. While this may not hold in case of a car driving closely behind a large truck, this case is rare if all vehicles maintain a safe following distance. Further, the bridge scenario limits the impact of reflections. While reflections can be beneficial (c.f. Fig. 2), they may also cause interference.

As shown in Fig. 3, we can compute the contact time equivalently to the case in Eq. 1. To this end, we only need to translate the angles from the horizontal plane to a vertical plane. In Fig. 3, θ_t represents the elevation angle of the RSU and the ICU. Hence, the joint optimization of the elevation angle and the transmit beamwidth is obtained as in Eq. 4.

C. RSU within a Roundabout

In our third scenario, we study the placement of the RSU within a roundabout. The benefit in this case is that cars must slow down when driving in a roundabout, which increases the contact time. In particular, we place the RSU at the center of the roundabout and consider an omni-directional antenna to provide coverage in all directions. To compensate for the low gain of the omni-directional antenna, the car can use a highly directional receive antenna. In contrast to our other scenarios, this poses no limitation due to the geometry of the roundabout scenario—a narrow beamwidth does not reduce the contact time since the receive antenna is simply pointing towards the center of the roundabout. Given a roundabout of radius r, the contact distance is computed as in Eq. 5.

$$d_c(\theta_{\text{rsu}}) = 2\pi r\left(\frac{\theta_{\text{rsu}}}{360°}\right) \quad (5)$$

IV. Vehicular 60 GHz Testbed

Our 60 GHz software-defined radio (SDR) testbed allows us to obtain low-layer information such as BER, PER, and SNR. In contrast, related work using commercial hardware can only obtain high-layer information such as throughput. We customize a mm-Wave packet communication system based on GNU Radio and developed at RWTH Aachen [20]. We use this code along with a USRP X310 to generate a stream of 4-QAM modulated data. This data is sent to an external up-converter for transmission in the 60 GHz band. At the ICU, the receiver continuously listens to the channel. After a signal is detected, the receiver performs carrier-frequency offset (CFO) compensation, and decodes the signal. In order to differentiate between packets that are lost due to blockage and those that are received with errors, we do not discard packets that do not pass the cyclic redundancy check (CRC). Hence, missing packets are due to blockage. Moreover, we tag each frame with a unique identifier. This allows us to compare the received and the transmitted data to compute the BER for each frame.

A. Metrics

We define the following metrics to better illustrate and analyze the performance of mm-Wave vehicular communication:

- **Receive time:** Period of time during which the receiver gets packets, regardless whether they contain bit errors.
- **Contact time:** Period of time during which the receiver is able to receive correct packets, that is, without bit errors.

In addition, we provide results for throughput, SNR, BER, and PER. Our current setup only supports 5 MHz bandwidth. Thus, we scale our results to 2 GHz, as defined in 802.11ad.

B. RSU Setup

The RSU (c.f. Fig. 4) consists of a desktop PC, a USRP X310, and a SiversIMA FC1005V/00 60 GHz up-converter. The computer generates the baseband signal, and sends it to the USRP via Gigabit-Ethernet. The USRP upconverts the signal to an intermediate frequency (IF) of 1.6 GHz that is then fed to the SiversIMA to be upconverted and transmitted in the 60 GHz band. To transmit the signal, we use either a horn antenna (7°, 20°, or 80°), or an omni-directional antenna.

C. ICU Setup

The ICU is comprised of the same elements as the RSU, and is placed on the front passenger seat of a BMW 3-Series car. We receive the incoming signal with a horn-antenna (7°, 20°, or 80°) attached to a SiversIMA FC1005V/00 converter. We feed the output of the converter to a USRP X310, which in turn sends the baseband signal to a laptop computer. To power all of these devices in the car, we use an additional car battery connected to a power converter that provides a regular alternate current power supply. Fig. 5 depicts our car setup.

D. Location

We temporarily installed the RSU at multiple locations in the city of Leganés, Spain. All experiments were carried out under real traffic conditions at the beginning of August 2016.

Fig. 4: RSU setup in the bridge scenario.

Fig. 5: ICU from outside (left) and inside (right) the car.

V. Results

In this section, we present the results obtained from our vehicular 60 GHz testbed described in Section IV. We consider the three scenarios described in Section III, namely, at the road side, on top of a bridge, and within a roundabout. Additionally, we consider a static case in which we analyze whether the 60 GHz signal can penetrate through one or more cars parked side by side. This allows us to assess the impact of blockage among cars driving in parallel lanes on, e.g., a freeway.

A. RSU at the Road Side

For our first experiment, we place the RSU next to a pedestrian crossing on a double lane road. We point the antenna of the RSU at $\theta_t = 45°$, and the antenna of the ICU at $\theta_t = 0°$. That is, the RSU points towards the cars approaching the pedestrian crossing, and the ICU points in the direction of the car movement. We set both θ_t to different values since the car structure blocks the signal if we set the

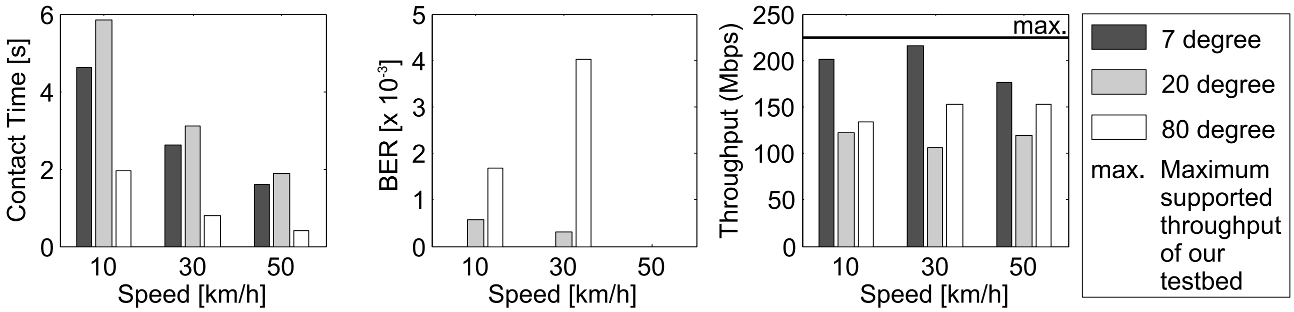

Fig. 6: Road Side Scenario. Average contact time, BER, and throughput out of multiple experiment repetitions.

ICU at 45° (c.f. Fig. 5). We measure performance for three different speeds (10 km/h, 30 km/h, and 50 km/h) and for three different antenna beamwidths (7°, 20°, and 80°). For each experiment, we use the same beamwidth at the RSU and at the ICU. Further, we drive the car on the right lane of the double lane road to avoid disturbing traffic, in particular when driving at 10 km/h only.

Fig. 6 depicts our results in terms of contact time, BER, and throughput for this scenario. As discussed in Section III, the contact time decreases with speed—the faster the car, the less time the transmit and the receive beams are aligned. However, we observe that the antenna beamwidth plays a significant role in this case. While the contact time increases as expected when switching from 7° to 20°, it decreases again for 80°. The underlying reason is related to the antenna gains. Although the 80° antenna covers a wide angle, it has less gain than the more directive 20°. For the data transmission to start, the car must be much closer to the RSU for 80° than for 20°, resulting in a much shorter contact time. This difference in terms of gain and directivity also impacts the BER and PER. For 7°, the narrow beamwidth only allows communication when the car is close to the RSU. Moreover, the high gain ensures that the signal reaches the ICU with high signal strength. As a result, we did not observe any packet errors in our 7° experiments. Accordingly, the BER in Fig. 6 increases the wider the beamwidth. Apparently, the BER decreases as the speed increases. However, the faster the car, the less packets are received, and thus the lower the probability that we observe bit errors, even if the BER is the same. Further, the better performance in terms of BER of narrow beamwidths translates into the 7° antenna achieving a higher throughput than the 20° and 80° antennas. The maximum throughput indicated with a line in Fig. 6 is given by the speed of the computers running GNU Radio at the RSU and ICU (c.f. Section IV), and is thus not an intrinsic limitation of our scenario. The slightly higher throughput of the 80° case compared to the 20° case suggests that the former is able to transmit more packets than the latter when the car is very close to the RSU due to its wider angle.

Next, we study the distribution of SNRs in Fig. 7. We observe that SNRs are mostly in the range from 15 dB to 20 dB. However, the higher the speed, the lower the SNRs. The reason for this behavior is that the road where we performed this experiment has bumps to force cars to slow down. As a

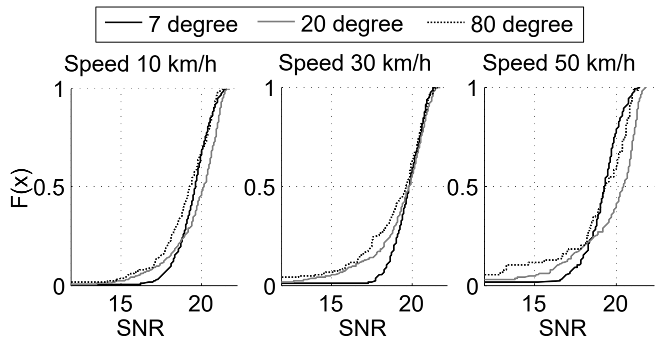

Fig. 7: SNR distribution in Road Side Scenario.

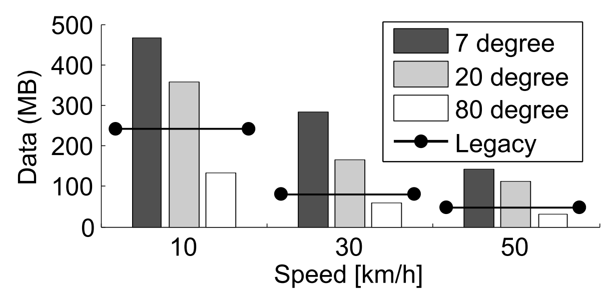

Fig. 8: Road Side Scenario. 60 GHz vs. legacy WiFi.

result, the antenna at the ICU bounced vertically at each bump, resulting in SNR fluctuations. We validate this observation in Section V-B, which considers a road without bumps and results in more stable SNRs. The results also show that the wider the beamwidth, the larger the variance of SNRs. This is expected in this scenario, since the wider the beam, the larger the coverage area of the RSU (c.f. Fig. 1). Thus, the ICU starts receiving data at a larger distance as it approaches the RSU, which inevitably results in lower SNRs.

Finally, in Fig. 8, we compare the performance of our 60 GHz fixed beamsteering approach to legacy 802.11p-like WiFi. For WiFi, we assume a circular range of 100 meters and a fixed rate of 27 Mbps [1]. The key benefit of WiFi is that the ICU can communicate with the RSU as long as it is within its range, that is, also after the car has passed by the RSU. As discussed above, the throughput in our testbed is limited due to hardware constraints. Hence, for the comparison in Fig. 8 we extrapolate our results in Fig. 6 assuming a maximum throughput of 900 Mbps, which is easily achievable with

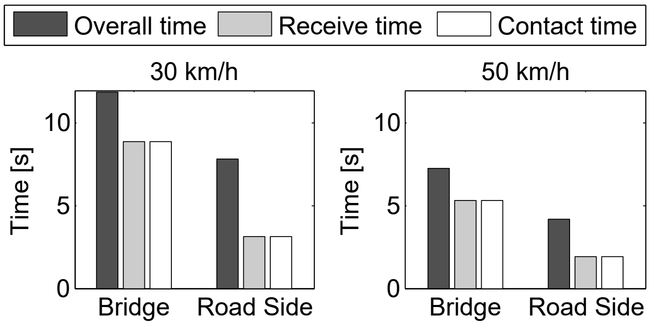

Fig. 9: Bridge vs. Road Side Scenario. Communication times.

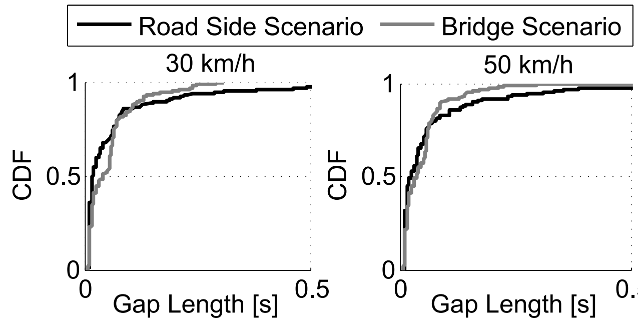

Fig. 11: Communication gaps (Bridge vs. Road Side Scenario).

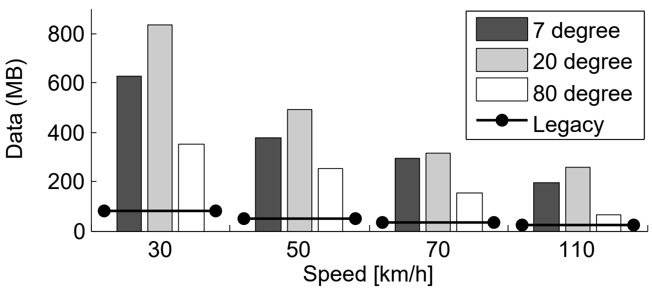

Fig. 10: 60 GHz vs. legacy WiFi in the Bridge Scenario.

commercial 60 GHz hardware [18]. Although the contact time for our 60 GHz approach is much shorter than for legacy WiFi, Fig. 8 shows that we achieve higher throughput. Interestingly, this only holds for *narrow* beamwidths. Hence, we conclude that short but very high throughput transmissions are more beneficial than long but low throughput alternatives. In other words, short contact times are not necessarily a limitation.

B. RSU on Top of a Bridge

In our second experiment, we place the RSU on top of a bridge crossing a two lane road (c.f. Fig. 4). We set $\theta_t = 45°$ at both the RSU and the ICU. That is, the RSU points at an angle of $45°$ down to the road, and the ICU points at an angle of $45°$ up to the bridge through the windshield of the car. The road allows for higher speed than our location in Section V-A, and thus we measure performance for 30 km/h, 50 km/h, 70 km/h, and 110 km/h. Regarding beamwidths, we consider again $7°$, $20°$, and $80°$ antennas, using the same for RSU and ICU.

We expect to achieve higher contact times in our bridge scenario compared to the road side case, since the elevated position of the RSU allows to start the communication much earlier. Indeed, Fig. 9 shows that the contact time for the bridge case is more than double than that in Section V-A for both 30 km/h and 50 km/h. Further, the relative difference between the overall communication time and the actual contact time is less. The former is the time interval from the first to the last packet, including any communication gaps due to, e.g., antenna misalignments. That is, the communication is significantly more stable in the bridge scenario than in the road side case. This is partially related to the lack of bumps, as discussed earlier. Moreover, we observe that in both scenarios the difference between the receive time and the contact time is minimal, which means that our receiver successfully decodes most of the packets that it receives during the experiment.

The larger contact time naturally increases the amount of data that the RSU can transmit compared to the road side case, as shown in Fig. 10 compared to Fig. 8. This also increases the gain of our 60 GHz approach compared to a legacy WiFi system, delivering up to $11\times$ more data to the ICU despite the directionality of the communication. However, in contrast to the road side scenario, in this case an intermediate beamwidth of $20°$ delivers the most data. Intuitively, this occurs because the increase in contact time when switching from a $7°$ to a $20°$ antenna is much larger from the top of a bridge than from the road side. In terms of the equations in Section III, the underlying reason is that parameter l is significantly larger in the bridge case than in the road side case. As a result, the benefit of transmitting for a longer period of time outbalances the benefit of using the narrower $7°$ antenna.

Next, we compare the impact of the road bumps in the road side scenario with the even road in the bridge case. In Fig. 11 we depict the distribution of the communication gaps during the overall communication time. Such gaps occur when antennas are temporarily misaligned due to, e.g., a bump. We observe that the gaps for the road side scenario are typically larger than for the bridge case. In particular, the maximum gap length is significantly larger in the road side case. Further, in Fig. 12 we depict the SNR fluctuations during one contact time for different speed and antenna beamwidth settings in both scenarios. We observe that the even bridge case is significantly more stable than the road with bumps, in-line with our earlier results. Most interestingly, fluctuations become smoother for the $80°$ antenna compared to the $20°$ case. Since the beam is wider in the former case, shakiness has less influence.

C. RSU within a Roundabout

Our third experiment considers an RSU placed at the center of a roundabout. We use an omni-directional antenna at the RSU, and $7°$, $20°$, and $80°$ horn antennas at the ICU. We place the ICU on the passenger seat but point it to the window on the driver's side, such that it points towards the RSU when the car is in the roundabout. Thus, the driver is seated between the RSU and the ICU. However, the transmitter is slightly closer to the windshield than the head of the driver. As a result, we

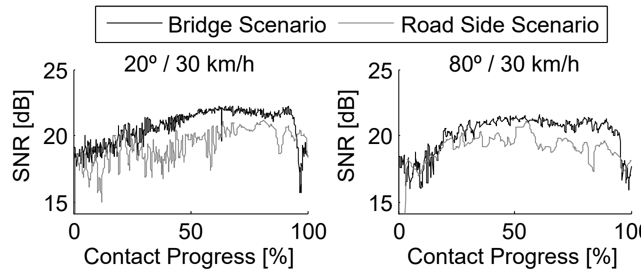

Fig. 12: SNR fluctuations bridge case vs. road side case. The "contact progress" reflects the normalized contact time.

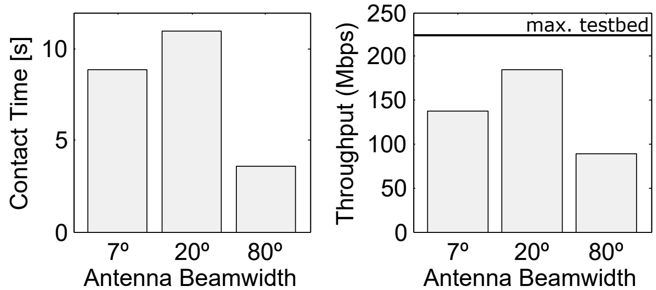

Fig. 13: Contact time and throughput in roundabout scenario.

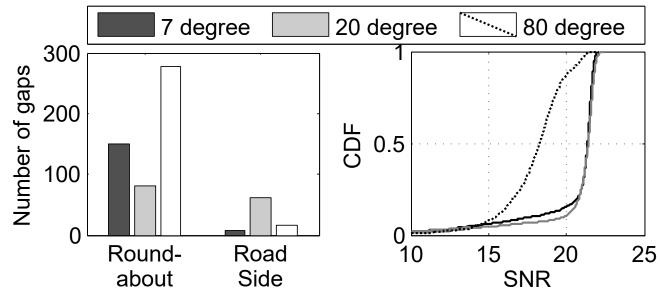

Fig. 14: Communication gaps and SNR in roundabout case.

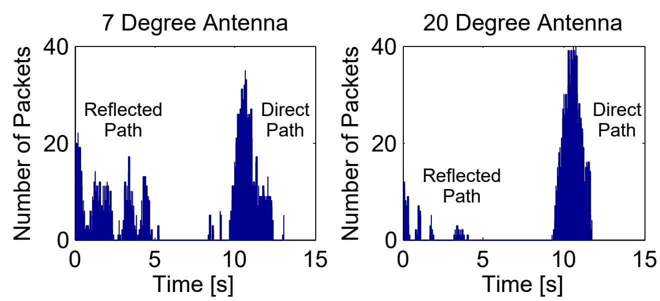

Fig. 15: Reflection off nearby wall in roundabout scenario.

did not observe any noticeable blockage. In our experiments, the speed inside the roundabout is limited to roughly 30 km/h.

Intuitively, we expected the contact time to be independent of the beamwidth (c.f. Section III-C). However, Fig. 13 shows that this does not fully hold. In particular, the contact time of the 80° antenna is much lower than for 7° and 20°. This is most likely due to the low gain of the 80° antenna, and the uneven radiation pattern of the omni-directional antenna. That is, the contact time for the 80° case is lower because the RSU often cannot reach the ICU due to path loss. The ICU only receives data when the car is driving through a roundabout section in which the omni-directional antenna has a peak of its radiation pattern. Our measurement logs reflect this behavior. Those logs also show that the 7° antenna looses connection earlier than the 20° when leaving the roundabout, yielding the shorter connection time in Fig. 13. As a result, the 20° antenna has slightly higher SNR, resulting thus in the highest throughput. Hence, we conclude that antenna beamwidth does play a role also in the roundabout case. Fig. 14 depicts the SNR distribution for all antennas, which clearly shows the aforementioned strong difference in terms of SNR of the 7° and 20° cases compared to the 80° antenna. This also results in a more frequent communication gaps for the 80° case (c.f. Fig. 14). Interestingly, the number of gaps is in general much higher than for other scenarios such as the road side case. This is probably due to the partial shadowing caused by the plants located inside the roundabout for decoration.

Additionally, we study the performance when placing the RSU outside the roundabout, pointing towards the center. In this case, we use a wide 80° antenna for transmission in order to cover as much area as possible of the roundabout. The antenna of the ICU is pointing at $\theta_t = 90°$, that is, through the passenger seat window. Hence, we expected to receive packets only when the car was passing next to the RSU. However, Fig. 15 shows that we also received packets when the car was at the opposite side of the roundabout. The underlying reason is that the signal reflected off a concrete wall at the other side of the roundabout, allowing the receiver to decode data via a reflected path. Hence, we conclude that reflections of nearby objects along the road can play a significant role.

D. *Road Side Reflections*

To get more insights on the impact of reflections, we consider a scenario as in Fig. 2. We place the RSU at the side of a residential single-lane road, and point it towards a parked car. At the ICU, we point the antenna towards the direction from which we expect to receive the reflection. We then drive at 20 km/h along the road until passing the RSU location.

Fig. 16 shows that the ICU is able to decode a significant number of packets as we drive past the reflected signal. After the main reflected burst is over, we often observe a few isolated packets. During our measurements, we confirmed that those isolated packets stem from the direct path that the car crosses after crossing the reflected path (c.f. Fig. 2). The number of packets for that second burst is very low since the ICU is pointing towards the row of parked cars. As expected, the length of the main burst increases with the antenna beamwidth, since the reflected path becomes wider. Still, the actual number of received packets is largest for the 20° antenna since it provides both a significant beamwidth and relatively high gain.

E. *Car Blockage*

Finally, we measure the PER in a static scenario for transmission at different heights through two and three cars

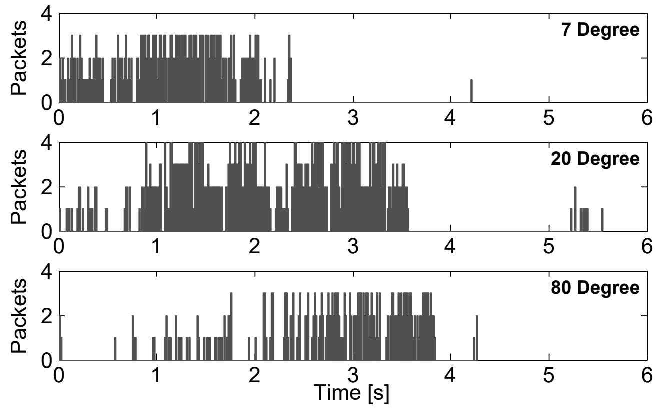

Fig. 16: Packets arriving at the ICU via a car reflection.

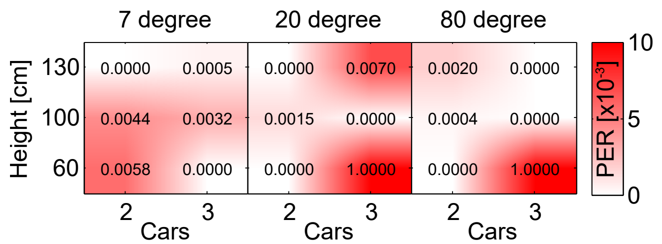

Fig. 17: PER for transmission through cars at multiple heights.

parked in parallel. Fig. 17 shows our results. As expected, we observe generally a higher PER for the case of three cars than for two cars only. Moreover, extreme cases with PER $= 1$ occur when the receiver is low, that is, when the signal would have to traverse the whole car body. Higher heights result in lower PER since the path is mostly blocked by window glass only. Wider beamwidths tend to yield better results since more reflective paths become feasible. However, the reduced antenna gain occasionally results in very high PER values. In contrast, the $7°$ antenna is never entirely blocked but tends to yield non-zero PER values. We conclude that transmission through parallel cars is feasible but can easily result in link loss.

VI. Conclusions

We present a simple yet effective scheme to deal with the need for directional communication in mm-Wave infrastructure to vehicle networks. We exploit the fact that the road geometry and the arrival direction of cars are known in vehicular scenarios in order to compute *fixed* beamsteering and beamwidth angles that are suitable for the average case. Hence, no costly beam training is needed for each car approaching an RSU. We build a first-of-its-kind SDR-based practical vehicular testbed that enables 60 GHz packet-level transmissions. Using this testbed, we show that our aforementioned approach is feasible and yields significant throughput gains compared to legacy 802.11p-based systems. We conclude that the high throughput in the 60 GHz band compensates for the short contact times resulting from directionality. This paves the way for 60 GHz vehicular networks.

Acknowledgements

This paper is supported by the European Research Council grant ERC CoG 617721, the Spanish Ministry of Economy and Competitiveness through grants Ramon y Cajal RYC-2012-10788 and HyperAdapt TEC2014-55713-R, the Madrid Regional Government through the TIGRE5-CM program S2013/ICE-2919, the LOEWE initiative (Hessen, Germany) within the NICER project, and the German BMBF within CRISP.

References

[1] R. W. Heath, "Vehicular Millimeter Wave Communications: Opportunities and Challenges," available at http://users.ece.utexas.edu/ rheath/presentations/2015/DSTOPvehicularMmWave2015Heath.pdf.

[2] N. González-Prelcic, R. W. Heath, and J. M. El MalekVázquez, "V2X Communications: The Killer Application of Millimeter Wave," available at http://networld2020.eu/wp-content/uploads/2016/03/S03P02_V2X_mmWave.pdf.

[3] P. Kumari, N. González-Prelcic, and R. W. Heath, "Investigating the IEEE 802.11ad Standard for Millimeter Wave Automotive Radar," in *IEEE VTC Fall*, 2015.

[4] J. Choi, N. G. Prelcic, R. C. Daniels, C. R. Bhat, and R. W. H. Jr., "Millimeter Wave Vehicular Communication to Support Massive Automotive Sensing," *CoRR*, vol. abs/1602.06456, 2016.

[5] T. Nitsche, A. B. Flores, E. W. Knightly, and J. Widmer, "Steering with Eyes Closed: mm-Wave Beam Steering without In-Band Measurement," in *IEEE INFOCOM*, 2015.

[6] G. Sim, A. Loch, A. Asadi, V. Mancuso, and J. Widmer, "5G Millimeter-Wave and D2D Symbiosis: 60 GHz for Proximity-based Services," *IEEE Communications Magazine*, 2016.

[7] T. S. Rappaport, S. Sun, R. Mayzus, H. Zhao, Y. Azar, K. Wang, G. N. Wong, J. K. Schulz, M. Samimi, and F. Gutierrez, "Millimeter Wave Mobile Communications for 5G Cellular: It Will Work!" *IEEE Access*, 2013.

[8] G. H. Sim, A. Asadi, A. Loch, M. Hollick, and J. Widmer, "Opp-Relay: Managing Directionality and Mobility Issues of Millimeter-Wave via D2D Communication," in *IEEE COMSNETS*, 2017.

[9] J. Blumenstein, T. Mikulasek, A. Prokes, T. Zemen, and C. Mecklenbrauker, "Intra-Vehicular Path Loss Comparison of UWB Channel for 3-11 GHz and 55-65 GHz," in *IEEE ICUWB*, 2015.

[10] E. Ben-Dor, T. S. Rappaport, Y. Qiao, and S. J. Lauffenburger, "Millimeter-Wave 60 GHz Outdoor and Vehicle AOA Propagation Measurements Using a Broadband Channel Sounder," in *IEEE GLOBECOM*, 2011.

[11] Y. Kim, H.-Y. Lee, P. Hwang, R. K. Patro, J. Lee, W. Roh, and K. Cheun, "Feasibility of Mobile Cellular Communications at Millimeter Wave Frequency," *IEEE Journal of Selected Topics in Signal Processing*, 2016.

[12] R. J. Humpleman and P. A. Watson, "Investigation of Attenuation by Rainfall at 60 GHz," *Proceedings of the Institution of Electrical Engineers*, 1978.

[13] H. Xu, T. S. Rappaport, R. J. Boyle, and J. H. Schaffner, "Measurements and Models for 38-GHz Point-to-multipoint Radiowave Propagation," *IEEE JSAC*, 2000.

[14] Z. Qingling and J. Li, "Rain attenuation in millimeter wave ranges," in *Symposium on Antennas, Propagation, and EM Theory*, 2006.

[15] Y. Zhu, Z. Zhang, Z. Marzi, C. Nelson, U. Madhow, B. Y. Zhao, and H. Zheng, "Demystifying 60GHz Outdoor Picocells," in *ACM MobiCom*, 2014.

[16] S. Sur, V. Venkateswaran, X. Zhang, and P. Ramanathan, "60 GHz Indoor Networking Through Flexible Beams: A Link-Level Profiling," *ACM SIGMETRICS Performance Evaluation Review*, 2015.

[17] S. Sur, X. Zhang, P. Ramanathan, and R. Chandra, "BeamSpy: Enabling Robust 60 GHz Links Under Blockage," in *USENIX NSDI*, 2016.

[18] A. Loch, I. Tejado, and J. Widmer, "Potholes Ahead: Impact of Transient Link Blockage on Beam Steering in Practical mm-Wave Systems," *European Wireless*, 2016.

[19] M. K. Haider and E. W. Knightly, "Mobility Resilience and Overhead Constrained Adaptation in Directional 60 GHz WLANs: Protocol Design and System Implementation," in *ACM MobiHoc*, 2016.

[20] J. Arnold, L. Simic, M. Petrova, and P. Mähönen, "Demo: Spectrum-Agile mm-Wave Packet Radio Implementation on USRPs," in *Workshop on Software Radio Implementation Forum*, 2015.